

Qualitative Difference of Equilibrium Current between W7-AS and W7-X Configurations

YOKOYAMA Masayuki*

National Institute for Fusion Science, Oroshi-cho 322-6, Toki 509-5292, Japan

(Received: 5 December 2000 / Accepted: 18 August 2001)

Abstract

The equilibrium current (EC) is examined to clarify qualitative difference between Wendelstein 7-AS (W7-AS) and Wendelstein 7-X (W7-X) based on the geometrical factor (G_{EC}) defined with Boozer magnetic spectrum. The dipole EC (DEC) in W7-X is significantly reduced with the reduction of poloidal inhomogeneity of B and higher rotational transform compared to those of W7-AS. The amplitude of the helical EC (HEC) is about the half of DEC in W7-X, which is qualitatively different from the predominancy of DEC in W7-AS. This comparable amplitude between DEC and HEC is the unique feature of the W7-X, which has not been the case for non-symmetric stellarator configurations.

Keywords:

equilibrium current (EC), geometrical factor, W7-AS, W7-X, dipole and helical EC

1. Introduction

The successful experiments performed in “partly optimized” W7-AS [1] have given several experimental basis for the “fully optimized” W7-X [2], which has been optimized based on several physical criteria [3]. One of those criteria is the reduction of Pfirsch-Schlüter (PS) current (or dipole EC, DEC) to improve equilibrium conditions with reducing Shafranov shift [2]. This concept has been already experimentally verified in W7-AS [2,4-6] with the demonstration of the reduction of Shafranov shift to the level of about the half of an equivalent conventional stellarator. Here, a “conventional stellarator” is defined as a stellarator configuration with poloidal inhomogeneity of the magnetic field strength, B , (let us call this PIB henceforth) almost equal to the geometrical inverse aspect ratio, A_p^{-1} . The W7-X has a higher rotational transform (ι) and further reduction of PIB to realize further reduction of DEC. The qualitative difference is that the helical inhomogeneity of B (HIB) appears in W7-X largely than PIB. In this paper, EC properties are

examined in W7-AS and W7-X systematically based on magnetic spectrum in Boozer coordinates [7]. It should be noted that the existence of non-dipole EC in W7-X has already been pointed out in Ref. [8] with the computation of B produced by plasma currents of a finite beta equilibrium by NESTOR code. Based on the analysis in this paper, the relative amplitude between HEC and DEC can be simply obtained.

This paper is organized as follows. In Sec. 2, EC in three dimensional (3D) configurations is briefly explained. Those properties are compared between W7-AS (two configurations with different ι values) and W7-X in Sec. 3, where EC property is also compared to W7-AS experimental results [2] to assure this analysis. Finally, summary is given in Sec. 4.

2. EC in 3D Magnetic Configurations

The EC and PS diffusion in 3D magnetic configurations [10] is briefly explained as a basis of this study. The Boozer coordinates (s, θ_B, ζ_B) are exploited

*Corresponding author's e-mail: yokoyama@LHD.nifs.ac.jp

to analyze various configurations. Here s denotes the normalized flux surface label and (θ_B, ζ_B) the (poloidal, toroidal) angles, respectively. The covariant and contravariant representations of the magnetic field vector, \mathbf{B} , and equilibrium equation, $\nabla P = \mathbf{J} \times \mathbf{B}$, lead to the expression for the parallel component of the current density, J_{\parallel} , as

$$\frac{J_{\parallel}}{B} = \frac{1}{\bar{B}^2} \frac{dP}{ds} \sum_{m,n} \frac{nMI + mg}{nM - \iota m} \delta_{m,n}(s) \cos(m\theta_B - nM\zeta_B). \quad (1)$$

Here P is a scalar plasma pressure, M the toroidal field period number, $2\pi g(s)/\mu_0$ and $2\pi I(s)/\mu_0$ are total poloidal current outside a flux surface and total toroidal current density inside a flux surface, respectively. The $\delta_{m,n}$ is Fourier component of $1/B^2$ with $m(n)$ being the poloidal (toroidal) mode numbers. It is noted that n is expressed in the unit of M .

3. Comparison of EC between W7-AS and W7-X

The Shafranov shift in W7-AS has been measured such as with soft-X ray diagnostics [4] and magnetic measurements [5]. The results have shown a good agreement with calculations based on equilibrium code (such as NEMEC [11]) [4,6], which demonstrates the reduction of about factor two compared with a conventional stellarator as predicted. This good agreement has given a proof to the concept of EC reduction, which is further pursued in the design of W7-X [2].

The horizontal shift in the W7-AS induced from X ray profile analysis has been shown systematically in Fig. 12 in Ref. [2] as a function of volume averaged beta value, $\langle\beta\rangle$, for configurations with different ι values: $\iota \sim 1/2$ and $1/3$. The almost linear dependence of the horizontal shift on $\langle\beta\rangle$ both for experimental and calculation results for low beta range may imply that the EC property largely depends on the vacuum magnetic configuration where magnetic field does not change so much from that at vacuum configuration. If there is a strong dependence of $\sum_{m,n} \frac{nMI + mg}{nM - \iota m} \delta_{m,n}(s) \cos(m\theta_B - nM\zeta_B)$ on $\langle\beta\rangle$ in Eq. (1), the dependence of the horizontal shift on $\langle\beta\rangle$ might be no longer linear. Therefore, only vacuum magnetic configurations are considered henceforth to compare EC properties in W7-AS and W7-X. It is noted that the finite beta modification of magnetic field structure is suppressed significantly in W7-X so that this limited consideration would give rather accurate estimate even for high beta equilibria in W7-X.

The following geometrical parameter is introduced to evaluate EC as ($M = 5$ for W7-AS and W7-X)

$$G_{EC} = \sum_{m,n} G_{EC(m,n)}(s) \cos(m\theta_B - 5n\zeta_B) = \sum_{m,n} \frac{m}{5n - \iota m} \delta_{m,n}(s) \cos(m\theta_B - 5n\zeta_B). \quad (2)$$

Here, nMI is omitted because $mg \sim mR_0\bar{B} \gg nMI \sim nMaB_{\theta}$ typically holds, where B_{θ} is the poloidal magnetic field and $R_0(a)$ the major (minor) radius. The factor g is not included to exclude differences in R_0 and \bar{B} to compare different devices. The Fourier components, $G_{EC(m,n)}s$, are calculated based on $\delta_{m,n}s$ obtained by the Fourier decomposition of $1/B^2$ in the Boozer coordinates. Figure 1 shows Fourier spectrum of G_{EC} . Figures 1(a) and 1(b) are for cases with $\iota \sim 0.34$, 1(b) $\iota \sim 0.52$ both for W7-AS and 1(c) $\iota(0) \sim 0.84$ for W7-X, respectively. The first two cases correspond to the representative configurations for W7-AS. The configuration is characterized with ι value since ι is almost radially constant. The last case corresponds to the standard high-mirror configuration shown in Ref. [12]. The ι varies from $\iota(0) \sim 0.84$ to $\iota(1) \sim 1.0$. Let us, first, compare two configurations of W7-AS. The PIB is reduced about the half of A_p^{-1} in W7-AS, which gives $\delta_{1,0}$ of about 0.11 regardless to ι values. The difference of the amplitude of $G_{EC(1,0)} = -\delta_{1,0}/\iota$ is due to the difference of the connection length. The excellent agreement between experimental and calculation results for the horizontal shift in the case of $\iota \sim 1/2$ has been obtained in Ref. [2]. In Ref. [2], the measured horizontal shift is plotted as a function of $\langle\beta\rangle$, in which the slope corresponds to the degree of the horizontal shift for a unit $\langle\beta\rangle$. Therefore, let us consider that $G_{EC(1,0)}$ (1) in Fig. 1(b) gives the slope for the case of $\iota \sim 1/2$ shown in Ref. [2] (cf., Fig. 2 in this paper). This is because the horizontal shift which is proportional to the parallel current density (cf., Eqs.(1) and (2)). It is noted that $G_{EC(2,0)}$ does not arise the horizontal shift since its contribution is equal between innerside and outside of a torus. Based on this correspondence for the case of $\iota \sim 0.52$, the slope expected from $G_{EC(1,0)}$ (1) for the case of $\iota \sim 0.34$ is also shown in Fig. 2 (about 2/3 of that for the case of $\iota \sim 0.52$), which closely reproduces experimental data points shown in Ref. [2] (within about 10% deviation). This rather good agreement between experimentally measured horizontal shift for different ι cases in W7-AS and G_{EC} analysis is considered to assure this analysis.

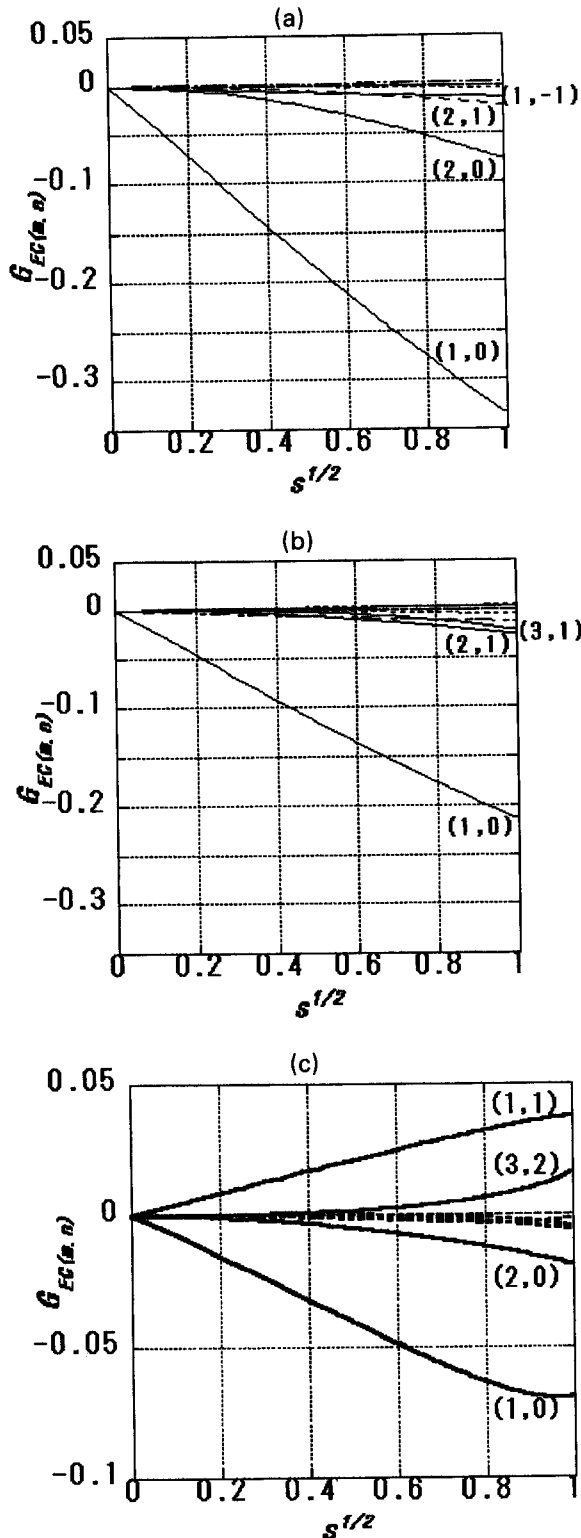


Fig.1 Fourier components $G_{EC(m,n)}$ in the Boozer coordinates for (a) $\tau \sim 0.34$, (b) $\tau \sim 0.52$ both for W7-AS and (c) standard high-mirror configuration [12] ($0.84 < \tau < 1.0$) for W7-X.

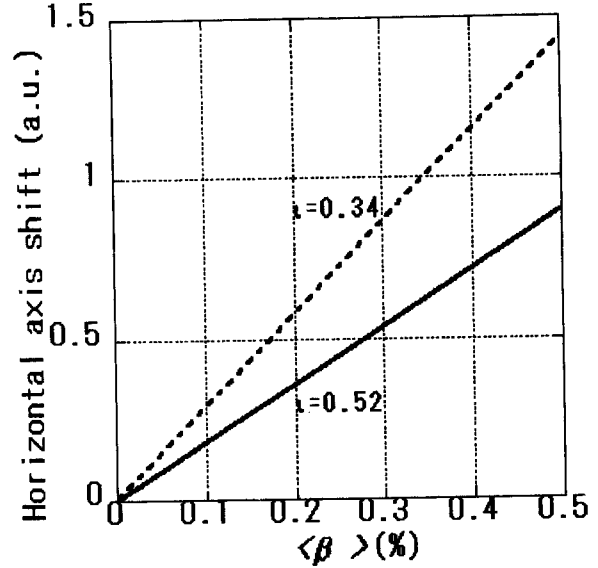


Fig. 2 The expected horizontal axis shift (a.u.) is shown for configurations with $\tau \sim 0.34$ and $\tau \sim 0.52$ in W7-AS. This is based on the correspondence of $G_{EC(1,0)}$ (1) in the configuration with $\tau \sim 0.52$ to the slope for $\tau \sim 1/2$ case shown in Fig. 12 of Ref. [2].

The $G_{EC(1,0)}$ is further reduced in W7-X due to the further reduction of PIB [2] (less than the half of A_p^{-1}) and higher τ . Moreover, the remarkable feature in W7-X is that HEC becomes apparent such as $G_{EC(1,1)}$ and $G_{EC(3,2)}$ (cf., Fig. 1(c)). Especially, the amplitude of $|G_{EC(1,1)}|$ is about the half of $|G_{EC(1,0)}|$ throughout a plasma. This comparable amplitude between DEC and HEC is the unique feature in the W7-X, which has been not the case in previous non-symmetric stellarator configurations. The $G_{EC(1,1)}$ contributes to EC with the same poloidal angle dependence as that of dipole component, $G_{EC(1,0)}$, at bean shaped cross section ($\zeta_B = 0$) with the opposite sign of amplitude since $\cos(\theta_B - 5\zeta_B)$ becomes $\cos\theta_B$. This is effective to suppress EC there. The contribution of $G_{EC(1,1)}$ changes its sign at triangular cross section ($\zeta_B/(2\pi/5) = 0.5$), which enhances EC there. It is noted that this HEC is anticipated to give little net vertical field to shift the magnetic axis due to its reversal along a helical direction. This statement can also be confirmed in quasi-helically symmetric (QHS) configuration [13] where HEC is predominant with DEC being negligibly small. Little change of magnetic axis position is recognized there even at $\langle \beta \rangle \sim 50\%$ compared to that at vacuum case.

4. Summary

The equilibrium current (EC) properties have been examined for W7-AS and W7-X based on Boozer magnetic spectrum. The geometrical factor, G_{EC} , defined with Fourier component of $1/B^2$ and corresponding connection length for the inhomogeneity of B in the Boozer coordinates is essential.

The poloidal inhomogeneity of B (PIB) is reduced about the factor of two compared to the geometrical inverse aspect ratio (A_p^{-1}) in W7-AS regardless to ι values. The difference of the amplitude of $G_{EC(1,0)} = -\delta_{1,0}/\iota$ is due to the difference of the connection length for PIB. In W7-AS configurations, EC is almost dipole. The good agreement between experimentally measured Shafranov shift for different ι cases in W7-AS and G_{EC} analysis is considered to assure this analysis.

The $G_{EC(1,0)}$ is further reduced in W7-X due to the further reduction of PIB (less than the half of A_p^{-1}) and higher ι . The helical EC (HEC) also becomes apparent. Especially, the amplitude of $|G_{EC(1,1)}|$ is about the half of $|G_{EC(1,0)}|$ throughout a plasma. This comparable amplitude between DEC and HEC is the unique feature in the W7-X, which has not been the case in previous non-symmetric stellarator configurations.

Acknowledgements

The work presented here is based on W7-AS and W7-X equilibrium calculations, which has been possible with precise boundary shape for these configurations. Prof. J. Nührenberg and Dr. J. Geiger are gratefully acknowledged for allowing the author to use these required data and also fruitful discussions. This work has been also supported by grant-in-aid from the Monbusho.

References

- [1] H. Renner *et al.*, Plasma Phys. Control. Fusion **31**, 1579 (1989).
- [2] G. Grieger *et al.*, Phys. Fluids B **4**, 2081 (1992).
- [3] J. Nührenberg, in Int. Toki Conf. 1989 (Proc. 1st Int. Toki Conf., Toki, Japan), Proc-3, National Institute for Fusion Science, Nagoya, Japan, 29 (1990).
- [4] A. Weller *et al.*, Proc. 1990 Euro. Conf. on Control. Fusion and Plasma Phys., Amsterdam, Vol.14B, Part II, 479 (1990).
- [5] H. Renner *et al.*, Proc. 1992 Int. Conf. on Plasma Physics, Innsbruck, Vol.16C, Part I, I-501 (1992).
- [6] H. Callaghan, J. Geiger *et al.*, (Proc. 24th Eur. Phys. Conf. Berchtesgarden, 1997), Vol.21A, Part IV, Eur. Phys. Soc., 1617 (1997).
- [7] A. Boozer, Phys. Fluids **23**, 904 (1980).
- [8] P. Merkel, *Theory of Fusion Plasmas* (Proc. Workshop Varenna, 1987) Editrice Compositori, Bologna, 25 (1987).
- [9] D. Pfirsch and A. Schlüter, Report MPI/PA/7/62, Max-Planck Insitut (1962).
- [10] M. Wakatani, *Stellarator and Heliotron Devices*, Oxford University Press, New York (1998).
- [11] S.P. Hirshman *et al.*, Comput. Phys. Commun. **43**, 143 (1986).
- [12] C. Nührenberg, Phys. Plasmas **3**, 2401 (1996).
- [13] J. Nührenberg and R. Zille, Phys. Lett. A **129**, 113 (1988).